Note
Calculation of SAR for Transmit Coil Arrays

WEIHUA MAO, ZHANGWEI WANG, MICHAEL B. SMITH, CHRISTOPHER M. COLLINS

Center for NMR Research, H066, Department of Radiology, The Pennsylvania State University College of Medicine, 500 University Drive, Hershey, PA 17033

ABSTRACT: Transmit coil arrays allowing independent control of individual coil drives facilitate adjustment of the B_1 field distribution, but when the B_1 field distribution is changed the electric field and SAR distributions are also altered. This makes safety evaluation of the transmit array a challenging problem because there are potentially an infinite number of possible field distributions in the sample. Local SAR levels can be estimated with numerical calculations, but it is not practical to perform separate full numerical calculations for every current distribution of interest. Here we evaluate superposition of separate electric field calculations—one for each coil—for predicting SAR in a full numerical calculation where all coils are driven simultaneously. It is important to perform such an evaluation because the effects of coil coupling may alter the result. It is shown that while there is good agreement between the superimposed and simultaneous drive results when using current sources in the simulations, the agreement is not as good when voltage sources are used. Finally, we compare maximum local SAR levels for B_1 field distributions that are either unshimmed or shimmed over one of three regions of interest. When B_1 field homogeneity is improved in a small region of interest without regard for SAR, the maximum local SAR can become very high. Concepts Magn Reson Part B (Magn Reson Engineering) 31B: 127–131, 2007

KEY WORDS: MRI; transmit array; RF shimming; SAR; simulations; electric field

INTRODUCTION

Recent development of RF hardware with multiple variable voltage or current sources for MRI has allowed for unprecedented control of the RF magnetic (B_1) field distribution (*1–4*). But though specified individual coil currents can produce specifically tailored RF magnetic field distributions, they also alter the electric field and SAR distributions (*5*). Safety evaluation of such arrays becomes a challenging task because an infinite number of current distributions are possible in the array, and thus an infinite number of field and SAR distributions are possible in a given sample.

Though it should be possible to estimate the average SAR in the region of the subject exposed to the RF fields in an array experimentally much as it is done for RF coils currently, evaluation of the maximum local SAR levels is not straightforward. Numerical calculations can be used to evaluate SAR distributions and maximum local SAR levels (*6*), but a full numerical calculation of each current distribution of interest is impractical. Here we evaluate the accuracy of evaluating the SAR distribution induced

Received 13 July 2006; revised 5 December 2006; accepted 5 December 2006

Correspondence to: Christopher M. Collins; E-mail: cmcollins@psu.edu

Concepts in Magnetic Resonance Part B (Magnetic Resonance Engineering), Vol. 31B(2) 127–131 (2007)

Published online in Wiley InterScience (www.interscience.wiley.com). DOI 10.1002/cmr.b.20085

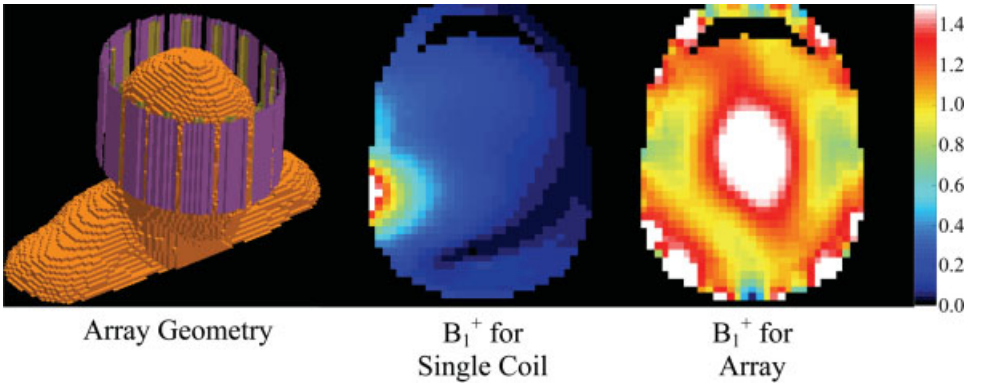

Figure 1 The geometry of the array modeled (left) and the magnitude of the circularly polarized component of the B_1 field pertinent to excitation (B_1^+) field when driving a single coil alone (center) and when driving all coils simultaneously (right). Linear color scale is from 0 to 1.5 μT.

by the array by superimposing electric fields from each individual coil at 300 MHz. Because coupling between coils can result in a complicated relationship between the drive of a certain coil at its terminals and the field it ultimately produces, this evaluation is necessary. We evaluate the accuracy of using this method of superposition both when using current sources and when using voltage sources. Finally, we present the SAR distributions of a transmit array when driven with four different current distributions of interest.

METHODS

A 3D digital human head model consisting of 23 different tissue types with a 5-mm isometric resolution was created with methods described previously (*7*). Two elliptical array coils containing 16 stripline TEM elements (*8*) were modeled and driven at 300 MHz. The coil geometries were identical to those modeled previously (*9*, *10*). The array geometry is shown in Fig. 1. As described previously (*9*), in each element of the array two current or voltage sources were used to connect the conductive element to the shield element, one at each end of each element.

To examine the accuracy of superimposing separate field calculations to calculate the SAR distribution induced when driving coils simultaneously, the RF field created while driving each element in the 16-element array separately with unit current or voltage sources was calculated using the finite-difference time-domain (FDTD) method with commercially available software (xFDTD; REMCOM; State College, PA). Then the resulting complex magnetic and electric fields from these 16 separate field calculations were added together and compared with another case where all elements were driven simultaneously in a single FDTD simulation. Here the phases of the sources followed the azimuthal angle positions of the coil elements. The comparison was performed both for using voltage sources and for using current sources in all 17 simulations.

We examined the SAR distribution of four current distributions of interest for the 16-element array. The desired current distributions were found using an optimization routine that capitalized on the superposition of the different magnetic fields (*9*, *10*). During

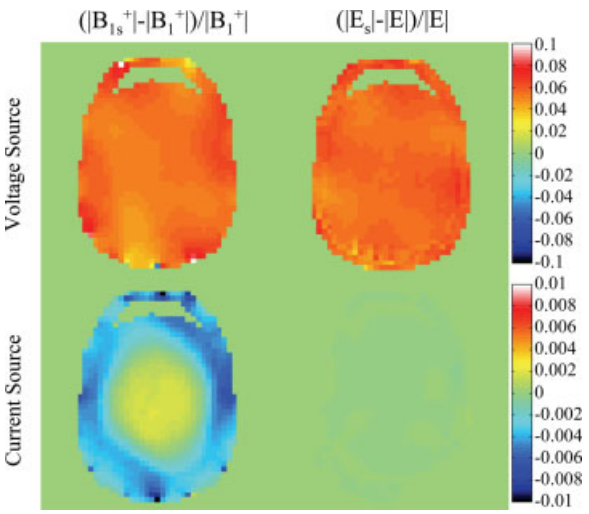

Figure 2 Relative difference between superimposed magnetic fields (B_{1s}^+) and superimposed electric fields (E_s) from 16 separate field calculations (with only one coil driven in each) and their counterparts (B_1^+ and E) from a single calculation when all 16 coils are driven simultaneously. When current sources are used (bottom), the error in using superposition is seen to be much lower than when voltage sources are used (top).

Table 1 Relative Difference of Magnetic Field and Electric Field Between Superimposed Fields From 16 Coils and a 16-Coil Array Under Different Driving Sources

	Relative Difference of $\|B_1^+\|$		Relative Difference of $\|E\|$	
Source Type	Average	Maximum	Average	Maximum
Voltage	0.0579	0.7735	0.0582	0.1149
Current	−0.0028	0.072	-5.0×10^{-5}	6.6×10^{-4}

optimization, the magnitude and phase of the separate coil currents were varied to produce a homogeneous distribution of the magnitude of the pertinent circularly polarized component of the B_1 field ($|B_1^+|$) over three different regions: (1) the entire head portion of the model, excluding neck and shoulders (optimizing whole head), (2) the entire brain including white matter, gray matter, and CSF (optimizing whole brain), and (3) a single axial slice of the brain (optimizing brain slice). After each optimization of $|B_1^+|$ homogeneity was performed, the resulting magnitudes and phases for all coils were used in a single FDTD calculation to determine the SAR with standard methods (*11*). For comparison, the $|B_1^+|$ and SAR distributions of an array with elements driven with a current pattern similar to that expected for a volume coil (standard drive) were also calculated.

RESULTS

The relative difference between the field distribution resulting from superposition of the separate field calculations and the field from a single calculation including all sources is shown in Fig. 2 on a single axial slice. The superimposed field is significantly different from the field of the array when using voltage sources, but they are almost identical when using current sources. As shown in Table 1, the average difference is less than 1% when current sources are used.

Figure 3 illustrates the normalized signal intensity distribution for a gradient echo image with a long TR (*9*, *10*) and SAR distribution during the pulse for the standard drive, whole-head optimized drive, whole-brain optimized drive, and single axial slice-optimized drive. The SAR can be high in some regions when using some optimized drive configurations. Table 2 lists the relative standard deviation of the B_1 field (standard deviation divided by the average) and average and maximum SAR values in the head model during the standard and optimized pulses. Because the average B_1^+ in the head portion of the model changes during optimization, the SAR values for field distributions like those in Table 2 and Fig. 3 but normalized as if to have the same average B_1^+ in the head are given in Table 3.

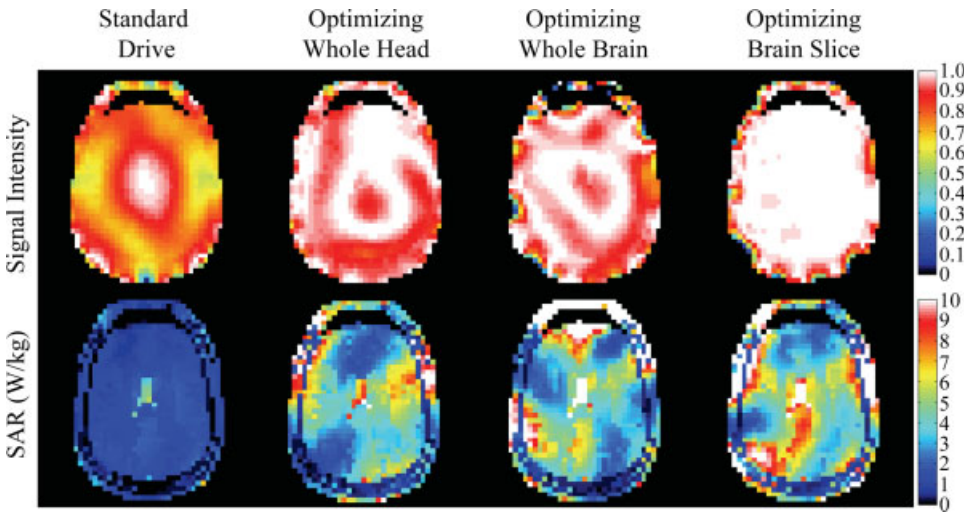

Figure 3 Signal intensity distribution and SAR levels (in each 5-mm-cubed voxel) on an axial plane through the center of the brain for four different field distributions of interest.

Table 2 Summary of SAR (W/kg) for a 16-Coil Array With Different Drives

	Standard Drive	Optimizing Whole Head	Optimizing Whole Brain	Optimizing Brain Slice
Relative Standard Deviation of B_1^+		0.26/0.12	0.17/0.06	0.13/0.006
Average SAR	0.58	2.34	3.25	3.66
Max. 1 g SAR	3.03	10.96	53.31	14.86
Max. 10 g SAR	2.58	6.81	11.41	10.03
Mean B_1^+ (μT) in head	0.99	1.61	1.84	1.91

DISCUSSION

RF fields can be manipulated by adjusting the driving current amplitude and phase of each coil individually. However, if the only objective is improvement of RF magnetic field homogeneity within a portion of the sample, other quantities may reach undesirable values. It has been observed that when the RF magnetic field is shimmed over a certain region, the RF magnetic field outside that region can become inhomogeneous (*9*). SAR should be taken into account as well. When the RF magnetic field homogeneity is optimized over a region the size of the brain or smaller, the maximum local SAR levels can reach extremely high levels, as seen in Table 2. The regions of highest SAR usually occur in a region with a highly inhomogeneous RF magnetic field. Where the RF magnetic field is homogeneous, the electric field tends to vary more gradually. Thus, when the RF magnetic field is shimmed over the entire head, rather than the brain or a single slice, the maximum local SAR levels tend to be lower (Table 2), though the field homogeneity is not as good (see Fig. 3, Table 2).

The calculated SAR extremes indicate that it would be valuable to consider the SAR or electric field when the driving condition of an array coil is optimized. Using the principle of superposition, both electric fields and magnetic fields can be calculated during a fast optimization routine, but this approach may not accurately account for coil coupling in general. In experiment, coils can be essentially decoupled for transmission purposes with a variety of methods, including the use of current sources (*12*). In simulations, when the electric fields driven by voltage sources are linearly summed, the mutual impedances between elements will lead to significant errors (see Fig. 1, Table 1). However, using current sources results in much lower error in use of the principal of superposition.

Though at least one initial attempt to consider SAR while optimizing magnetic field homogeneity with numerical calculations looks promising (*13*), the general application of such an approach is yet uncertain as local SAR levels and locations are patient specific (*14*, *15*) and it is not practical to create patient-specific numerical models of every patient before MRI imaging. The results in this article demonstrate that the superposition of electric and magnetic fields is valid when using current source driving methods, a fundamental step toward future developments of considering SAR for transmit arrays.

Table 3 Summary of SAR (W/kg) Normalized for 2 μT average B_1^+ in Head Portion of Model

	Standard Drive	Optimizing Whole Head	Optimizing Whole Brain	Optimizing Brain Slice
Average SAR	2.37	3.61	3.84	4.01
Max. 1 g SAR	12.37	16.91	62.98	16.29
Max. 10 g SAR	10.53	10.51	13.48	11.00

ACKNOWLEDGMENT

Funding for this work was provided by the National Institutes of Health through R01 EB 000454.

REFERENCES

1. Zhu Y, Watkins R, Giaquinto R, Hardy C, Kenwood G, Mathias S, et al. 2005. Parallel excitation on an eight transmit-channel MRI system. Proceedings of the 13th Annual Meeting of the ISMRM, Miami Beach. p 14.
2. Ullmann P, Junge S, Wick M, Ruhm W, Hennig J. 2005. Experimental verification of transmit SENSE with simultaneous RF-transmission on multiple channels. Proceedings of the 13th Annual Meeting of the ISMRM, Miami Beach. p 15.
3. Kurpad KN, Boskamp EB, Wright SM. 2005. A parallel transmit volume coil with independent control of currents on the array elements. Proceedings of the 13th Annual Meeting of the ISMRM, Miami Beach. p 16.

4. Hoult DI, Kolansky G, Kripiakevich D, King SB. 2004. The NMR multi-transmit phased array: a Cartesian feedback approach. J Magn Reson 171:64–70.
5. Angelone LM, Makris N, Vasios C, Wald L, Bonmassar G. 2006. Effect of transmit array phase relationship on local specific absorption rate (SAR). Proceedings of the 14th Annual Meeting of the ISMRM, Seattle. p 2038.
6. International Electrotechnical Commission (IEC). 2002. Medical electrical equipment part 2-33. Particular requirements for the safety of magnetic resonance equipment for medical diagnosis. IEC 60601 1-2-33:2002(E). Geneva: IEC.
7. Collins CM, Smith MB. 2001. Signal-to-noise ratio and absorbed power as functions of main magnetic field strength and definition of "90°" RF pulse for the head in the birdcage coil. Magn Reson Med 45:684–691.
8. Adriany G, Van de Moortele PF, Wiesinger F, Moeller S, Strupp JP, Andersen P, et al. 2005. Transmit and receive transmission line arrays for 7 Tesla parallel imaging. Magn Reson Med 53:434–445.
9. Mao W, Smith MB, Collins CM. 2006. Exploring the limits of RF shimming for high-field MRI of the human head. Magn Reson Med 56:918–922.
10. Collins CM, Liu W, Swift BJ, Smith MB. 2005. Combination of optimized transmit arrays and some parallel imaging reconstruction methods can yield homogeneous images at very high frequencies. Magn Reson Med 54:1327–1332.
11. Caputa K, Okeniewski M, Stuchly MA. 1999. An algorithm for computations of the power deposition in human tissue. IEEE Antennas and Propagation Magazine 41:102–107.
12. Nam H, Wright SM. 2006. Comparison of a current source and a voltage source in transmit SENSE. Proceedings of the 14th Annual Meeting of the ISMRM, Seattle. p 2563.
13. van den Berg CAT, van den Berg B, Kroeze H, Bartels LW, Lagendijk JJW. 2006. Simultaneous B1+ homogenization and SAR hotspot suppression by a phased array MR transmit coil. Proceedings of the 14th Annual Meeting of the ISMRM, Seattle. p 2039.
14. Liu W, Collins CM, Smith MB. 2005. Calculations of B1 distribution, specific energy absorption rate, and intrinsic signal-to-noise ratio for a body-size birdcage coil loaded with different human subjects at 64 and 128 MHz. Appl Magn Reson 29:5–18.
15. van den Berg B, van den Berg CAT, Kroeze H, Bartels LW, Lagendijk JJW. 2006. The effect of body size and shape on RF safety and B1 field homogeneity at 3T. Proceedings of the 14th Annual Meeting of the ISMRM, Seattle. p 2040.